CHAPTER 2

LITERATURE REVIEW

2.1. Introduction

Microwaves are serving our society in almost every action of day-to-day life. Most of the varieties of electronic products available, microwave tubes (electron-beam devices) still find its dominance for delivering high power (for civilian as well as defence) at microwave to sub-millimeter wavelength, and this is a property where their solid-state (technology beginning in the 1970's) counterparts are not able to compete because its scalability and efficiency issues. Microwave tubes, which operate essentially in high power, millimetre and sub-millimetre wave frequency regime, have continued to draw attention of system designer. Their applications are not only limited in plasma heating in fusion research but also in electronic warfare weaponary, long range and high resolution radars, high information density communication systems, strategic to industrial applications, generation of thermonuclear energy, medical applications and many more [Hirshfield *et al.* (1977), Flyagin *et al.* (1977), Andronov *et al.* (1978), Jory (1981), Gandhi (1981), Flyagin and Nusinovich (1988), Chu and Lin (1988), Gilmour Jr. (1986), Chu *et al.* (1990), Jain and Basu (1994), Basu (1996), Makowski (1996), Nusinovich (1999), Granatstein *et al.* (1999), Felch (1999), Thumm and Kasparek (2002), Thumm (2003), Sisodia (2003), Kartikeyan (2004), Du and Liu (2014)]. The beginning of microwave sources can be traced back to the first demonstrated the generation of 66cm wavelength electromagnetic waves by Heinrich Hertz in 1888 and that their property is almost same as ligth. His experiment proved that electrical signals could travel through open air (wireless) as also observed more than two decades earlier by James Maxwell [Hertz (1983)]. In 1893, Edison observed an electric current drawn between a heated filament and plate placed within an evacuated bulb, if the plate is held electrically positive with respect to the filament. The charge carriers

were later identified as negative electrons, whose existence was established by Thomson in 1897. In 1904, Fleming exploited the outcome of Edison's observation and used the diode (two terminal devices) as rectifier (AC to DC conversion) or detector of radio signals. In 1907, DeForest demonstrated that the flow of electrons from the cathode (filament) to anode (plate) can be controlled by a grid between the anode and cathode. However, when the operating wavelengths became comparable in size to the triode structural elements, the performance degraded sharply. This degradation is due to the electron transit time between the electrodes, the inductive reactance of the connecting wires and the capacitive admittance between electrodes. Minimization of the area of the electrodes and the length of the connecting wires can alleviate these problems, but this will ultimately limit the power handling capability of gridded tube. In the 1930's, it has been felt that distributed interactions between streaming electrons and co-traveling electromagnetic waves in resonant cavities and waveguides can solve the limitations of gridded tubes. Keeping this in mind, various conventional microwave devices has been invented during the 30-year interval, the "golden age" of microwave power tube research, beginning in the mid-1930s. One of the oldest members of the family of microwave tubes the smooth wall magnetron was developed in 1921 by Albert Hull. The importance of these microwave devices was immensely felt during the World War II which aroused needs to further explore the potentials of microwave tubes. This gave birth to the invention of cavity magnetron by K. Posthumas in 1935, and J. T. Randall and H. A. H. Boot in 1940, the klystron by the Varian brothers (Russell H. Varian and Sigurd F. Varian), W. C. Hahn, G. F. Metcalf, and William Hansen in 1939, and the traveling wave tube by N. E. Lindenblad in 1940, R. Kompfner in 1942, and J. R. Pierce and L. M. Field in 1947. In 1950s and 1960s, traveling wave tubes

and klystrons widely dominated the microwave tube industry [Gilmour Jr. (1986), Gandhi (1981), Sisodia (2006)].

In 1960, Nergaard proposed average power density as a figure of merit, providing an insightful basis for comparing device types and portraying trends in performance growth [Mourier (1961)]. The physical significance, as a figure of merit, derives from the fact that the maximum beam or charge carrier power that can be transported through a device is proportional to the circuit cross-sectional area, which is inversely proportional to the operating frequency. As the operating frequency is raised, these conventional microwave tubes fail to deliver high power at higher frequency. These requirements along with the growth in superconducting magnet technology improvements gave birth to a new class of microwave devices the fast-wave devices. The family of fast-wave devices includes gyromonotron [Lau *et al.* (1982), Timkin *et al.* (1982), Carmel *et al.* (1983), McDermott *et al.*(1983), Chu *et al.* (1985), Felch *et al.*(1986), Antonsen *et al.* (1986), Nusinovich *et al.* (1994), Dumbrajs and Nusinovich (2004), Glyavin and Luchinin (2007)], the gyro-klystron [Chu *et al.* (1985), Lawson *et al.* (1993), Choi *et al.* (1998), Blank *et al.* (1998)], and the gyro travelling-wave tube (gyro-TWT) [Chu *et al.* (1979), Seftor *et al.* (1979), Chu *et al.* (1980), Symon and Jory (1981), Lau *et al.* (1981), Granatstein *et al.* (1981), Barnett *et al.* (1981), Ahn (1982), Ganguly and Ahn (1984), Chu *et al.* (1990), Park *et al.* (1991), Leou *et al.* (1992), Park *et al.* (1994), Chu (1995), Wang (1995), Park *et al.* (1995), Leou *et al.* (1996), Rao *et al.* (1996), Wang *et al.* (1996), Gold and Nusinovich (1997), McDermott and Nusinovich (1998), Chu *et al.* (1998), Denisov *et al.* (1998), Leou *et al.* (1998), Felch *et al.* (1999), Chu *et al.* (1999), Nguyen *et al.* (2001), McDermott *et al.* (2002), Garven *et*

al. (2002), Yeh *et al.* (2003), Sirigiri *et al.* (2003), Chu (2004), Blank *et al.* (2005), Hung and Yeh (2005), Wang *et al.* (2011), Du and Lin (2014)].

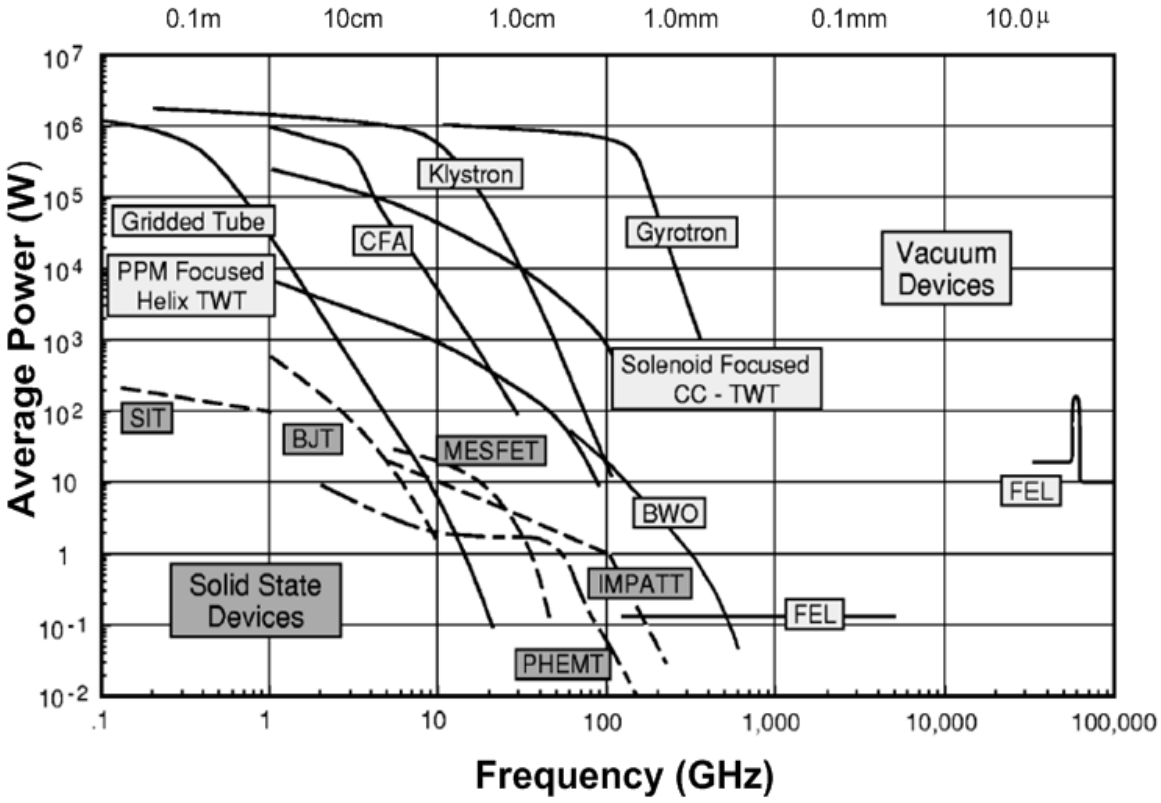

Figure 2.1. Comparison of average power versus frequency and wavelength for various types of devices [Parker *et al.* (2002)].

Finally, the gyro-oscillator and the FEL surpass slow-wave devices in the mid-1970 for high power at millimeter and sub-millimeter wave frequency range. The gyro-devices and FEL surpass the conventional slow-wave devices in the mid-1970 for high power at millimeter and sub-millimeter wave frequency range. In fact, the microwave tubes faced stiff competition from their solid state counterpart at some stage since the later was based on the highly developed semiconductor technology. Afterwards around seventies it was detained that the microwave tube technology would be replaced by the semiconductor device. However, the scenario has been changed in eighties with the growth of the

microwave tubes in terms of the performance. Miniaturised size of semiconductor devices at higher frequencies limits the power handling capability whereas in case of vacuum devices, size restriction is not an issue at the higher frequencies and it can delivers high output power with considerable power handling capability. The typical comparison of average power delivered by different devices has been represented in Fig. 2.1.

2.2. Classification of Microwave Tubes

Various kinds of instabilities can be present in a beam-wave system. Microwave tubes are classified on the basis of the principle of their operation. The operation of microwave tubes is broadly based on the principle of conversion of spontaneous radiation from individual electrons into coherent radiation. This is achieved in such devices by bunching the electrons in a proper phase with respect to the RF wave in the interaction structure by adjusting the device parameters, namely, the beam, background magnetic field and interaction structure parameters. The energy extraction process is unique to each of these instabilities. Different approaches to classifying the microwave tubes in described in literature [Basu (1996), Gilmour Jr. (1986), Gandhi (1981), Kartikeyan *et al*. (2013)]. In the first approach of microwave tubes are O-type and M-type tubes. (O is the short form of TPO standing for tubes à propagation des-ondes, and M is the short form of TPOM standing for tubes à propagation des ondes à champs magnetique). In the O-type tubes, the electrons move in the longitudinal direction due to a longitudinal magnetic field and interact with the longitudinal electric field supported by the interaction structure. The RF magnetic field does not take part in the beam-wave interaction mechanism of these devices. The interaction involves longitudinal space-charge wave and axial kinetic energy of the electron beam is converted into electromagnetic waves. In an M-type tube, the electrons

are subject to perpendicular DC electric and magnetic fields, and hence the device is also known as a crossed-field device. In this type, the transverse space-charge wave take part in the beam-wave interaction and the potential energy of the electron beam is converted into electromagnetic wave. For examples, traveling-wave tube and klystron belong to the O-type, and magnetron and crossed-field amplifier (CFA) belong to the M-type.

In the second approach, microwave tubes as the localized interaction and distributed interaction types of devices klystron, for example, belonging to the first type and traveling-wave tube to the second type in this approach.

In the third approach, microwave tubes are of the longitudinal interaction space-charge type to which traveling-wave tube and klystron belong, the transverse interaction space-charge type to which magnetron and CFA belong, and the cyclotron-mode interaction type to which gyrotron belongs.

In the fourth approach, we have two types: slow-wave and fast-wave types. Traveling-wave tubes and magnetrons are the examples of the first type, and gyrotrons and ubitrons are the examples of the second type.

In the fifth approach, microwave tubes may be classified as Cerenkov radiation, transition radiation, and bremsstrahlung radiation types. In the Cerenkov radiation type, electrons move in a medium with a speed greater than the phase velocity of electromagnetic waves in the medium. CFA and TWT belong to this type. In the case of transition radiation type, electrons pass through the boundary between two media with different refractive indices or pass through perturbations in a medium such as conducting grids and a gap between conducting surfaces. Klystron is an example of this kind. In the bremsstrahlung radiation type, radiation occurs when electrons move with an acceleration or deceleration in

electric and/or magnetic fields. Typically, these electronic movements are oscillatory. The electrons radiate coherent waves when the Doppler-shifted frequency of the wave coincides with the frequency of oscillation of electrons or with one of its harmonics. The examples of bremsstrahlung radiation type are: gyrotrons, ubitrons, peniotrons, and vircators (virtual cathode oscillators). In a gyrotron, the electron beam is made to be periodic by making electrons gyrate in a static magnetic field. In an ubitron, electrons are undulated by a wiggler magnetic field. In a vircator, electrons radiate while oscillating in a static electric field. It may be mentioned however that, though one try to classify microwave tubes into different types on the basis of interaction mechanism, it often becomes difficult to make a demarcation between the types. For instance, a klystron cavity of short length supports a spectrum of space-harmonic modes, a part of which corresponds to slow waves. So, such a transition radiation device may also be looked upon as a Cherenkov device. Similarly, one may consider a bremsstrahlung device, like, a slow wave cyclotron amplifier (SWCA) as a Cherenkov device [Basu (1996)].

Microwave tubes are able to fulfil the need of large power for radars with considerable efficiencies. Multi-octave bandwidth is provided by the microwave tubes (e.g., helix TWTs). For the communication purpose, microwave tubes are also able to provide moderate CW power, moderate bandwidth, high gain, high efficiency, etc. The realization of newer devices, such as, microwave power module (MPM) and micro-fabricated vacuum electronic tubes have added new dimensions to the microwave devices. These devices utilize the features of both solid state devices as well as vacuum electron beam devices. The MPM involves a solid-state power amplifier (SSPA), a wideband high-efficiency micro-TWT also known as vacuum power booster and a compact efficient

electronic power conditioner. The SSPA and the micro-TWT are responsible for the gain of MPM yielding high efficiency, improved noise- figure, less harmonic content, and reliable power amplifier. MPMs find applications in EW systems, phased array radars, weather radars, and communication systems [Joo and Choi (2005)].

2.3. Fast-Wave Gyrotron Devices

The transverse dimension of the interaction region of a gyro-device, like, the gyro-TWT decreases with frequency but not upto that extent as compared to a slow-wave device, like, TWT. Further, the fast–wave device can be operated at the higher-order modes, corresponding to higher eigenvalue, due to this reason the transverse dimension of a fast-wave device can be increased. It can handle a larger power at the higher frequencies due to a reduction in the power loss density at the walls of the RF structure. Further, the electron beam in a fast-wave device can be placed away from the walls of the RF structure to realize the larger field necessary for the proper beam-wave interaction. This also reduces the problem of beam interception at the wall of the metallic RF structure. In between the microwave and the optical frequencies, millimeter waves enjoy distinguishable advantages. The advantage of operating at higher frequencies is well understood for communication and radar applications. Optical frequencies is a better choice than either microwaves or millimeter waves on this count but the unfavorable effects of weather on free space optical communication has limited its role in long range wireless communication applications. Millimeter waves find extensive application in a wide range of communication and other applications. There exists a technological gap in the millimeter-wave range, no matter whether it is filled up by decreasing the frequency of quantum-mechanical devices like laser or by increasing the frequency of conventional microwave tubes [Gilmour (1986),

Nusinovich (2004)]. Energy of each quantum reduces, and retaining the population inversion becomes difficult in a quantum-mechanical device as the frequency is reduced. On the other hand, microwave tubes become tiny and hence its power output becomes reduced with the increase of frequency. This has led extensive search for electron devices for the generation and amplification of millimeter waves, in which the mechanism of conversion of spontaneous radiation to coherent radiation is based on electron cyclotron resonance maser (ECRM) instability and Weibel instability [Basu (1996]. The CRM mechanism dominates in the fast-wave devices while the Weibel mechanism is dominant in the slow wave devices. In CRMs the transverse energy of the electrons contained in the gyrations is converted to RF radiation, while the axial energy is left undisturbed.

In fast-wave gyro-devices, a hollow beam of electrons gyrating in helical paths interacts with the transverse electric mode of a fast-wave-guiding structure like a cylindrical waveguide, hence the name “fast-wave gyro-devices”. Classification of gyro devices is shown in fig. 2.2.

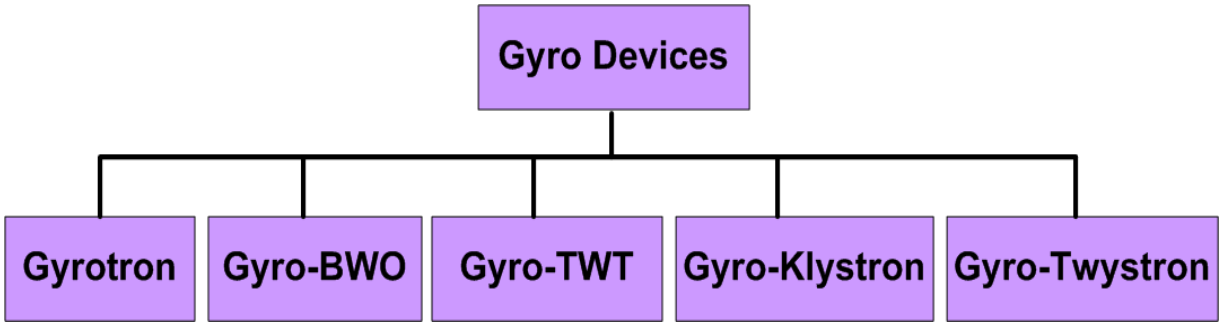

Figure 2.2. Classification of Gyro devices.

These devices are different from the conventional microwave tubes in that, here, basically the electron beam is made periodic rather than the interaction structure, which supports, in general, fast rather than slow electromagnetic waves. Transverse kinetic energy

of electrons is converted into electromagnetic energy rather than axial kinetic energy (as in a TWT) or potential energy (as in a magnetron) in microwave tubes. Cyclotron resonance for beam-wave interaction takes place when the Doppler-shifted frequency is nearly equal to the cyclotron frequency or any of its harmonics, unlike in a device like TWT where for such interaction the electron DC beam velocity is made synchronous with the RF phase velocity.The size of a fast-wave gyro-device is reduced with the operating frequency but not as much as that of a slow-wave device. On the other hand, taking a gyro-device operating close to the waveguide cutoff frequency of the waveguide mode with eigenvalue, being the cutoff wave number and the wall radius of the waveguide, we get the waveguide radius (representing the transverse dimension of the device) relative to the free-space wavelength. The fast-wave device enjoys an advantage with respect to the structure size over the slow-wave device, and obviously for higher order modes, we would get still greater advantage. Another advantage of a fast-wave gyro device structure like a cylindrical waveguide is that the electron beam could be placed far from the structure boundary to experience greater interaction field, unlike in the slow-wave device like TWT, in which the available field for interaction is stronger at the structure boundary. This relaxes the problem of interception of the electron beam by the metallic part of the device in a fast-wave gyro-device.

In CRM instability fast-wave gyro-devices like gyrotron, bunching of electrons is relativistic, unlike in a conventional slow-wave device like TWT. The electron bunch is positioned in the decelerating RF phase to ensure that most of the electrons interacting with RF waves transfer energy to rather than take energy from the latter. This is achieved in such a fast-wave gyro-device by slightly de-tuning the cyclotron resonance condition, unlike in a

slow-wave device like TWT, in which this is done by slightly offsetting the synchronism between the DC beam velocity and the RF phase velocity [Basu (1996), Kartikeyan *et al.* (20013)].

The concept of transverse kinetic energy conversion fast-wave gyro-devices has been derived from that of the corresponding axial kinetic energy conversion O-type devices like monotron, klystron, TWT, BWO, and twystron. Thus, the fast-wave gyro-device counterparts of these devices are gyro-monotron, or simply gyrotron, gyro-klystron, gyro-TWT, gyro-BWO, and gyro-twystron, respectively. In these devices CRM instability prevails over Weibel instability. Closely related to these devices are slow-wave cyclotron amplifier (SWCA), in which Weibel instability prevails over CRM instability, and cyclotron auto-resonance maser (CARM), in which these two instabilities are present in equal proportions.

2.4. Gyrotron Amplifiers

The advancement of overmoded amplifiers is more complicated than in the oscillator case because they should be kept stable in the absence of an input RF signal. Also, input couplers must be developed to inject the RF signal. Furthermore, performance parameters such as gain, bandwidth, phase stability, and noise become critically important. Gyro-amplifiers have large weight and volume than conventional amplifiers but they can provide significantly higher powers. The gyro-devices are divided in two groups, one oscillator and the other is amplifier. The gyromonotron (gyrotron) and gyro-BWO are the members of the first group. Devices like the gyroklystron, gyro-TWT, and gyro-twystron comes in the second group. These devices are analogous to their corresponding slow-wave counterpart's klystron, TWT, and Twystron. Gyro-devices are basically derived from gyrotron, but it is

not suitable for information carrying systems, due to its poor signal coherence and spectral quality. For communication system applications, amplifiers like gyroklystron, gyro-TWT or gyro-twystron are used. The RF interaction structures for these gyro-amplifiers are shown in Fig. 2.3.

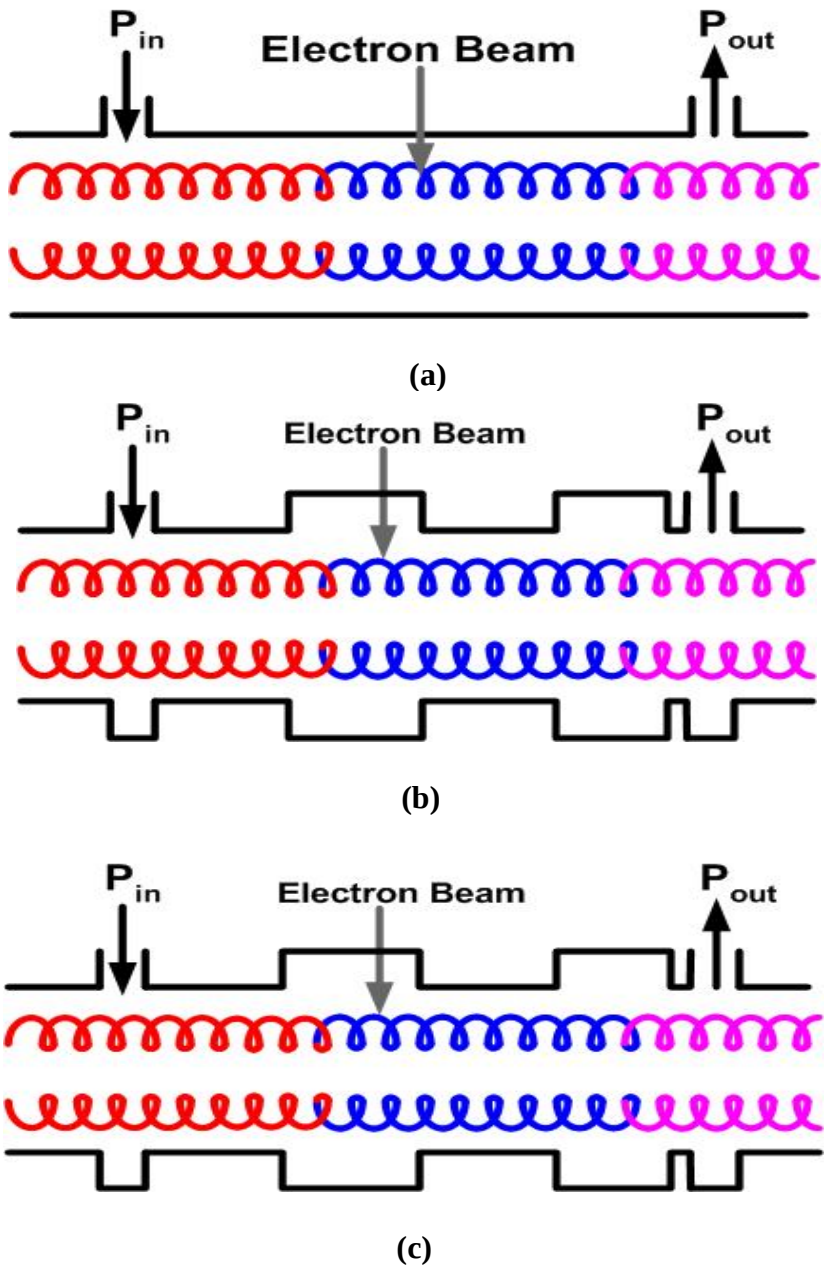

Figure 2.3. Interaction structures of different gyro-amplifiers **(a)** Gyro-TWT, **(b)** Gyroklystron, and (**c**) Gyro-Twystron.

2.5. Gyrotron TWT Amplifier

The gyro-TWT is a most promising high power (more than slow wave and laser devices) microwave and millimetre wave coherent radiation amplifier and working on the principle of electron cyclotron resonance maser (ECRM) instability. Gyro-TWT first described in 1958-1959 [Chu (2004)] and it used a resonant output cavity instead of an untuned travelling wave structure. The gyro-TWT mechanism was first studied experimentally using an intense relativistic electron beam (IREB) by Granatstein and his group [Granatstein *et al.* (1975)]. Due to near the matching of cyclotron mode and waveguide mode it has high gain and large bandwidth and because the group velocity is very close to beam electron velocity. The gyro-TWT amplifier is inherently capable high gain, wide bandwidth, short pulses and high phase sability. Through, gyro-TWT is a fast-wave travelling wave tube amplifier but in its conventional form, i.e., gyro-TWT using smooth wall cylindrical waveguide, does not possess wide band capability as its slow wave counterpart TWT amplifier does. Schematic of a gyro-TWT amplifier is shown in Fig 2.4. The gyro-TWT has the potential to generate high power over a wide range of frequencies in the millimetre and sub-millimetre wave band of the electromagnetic spectrum. The gyro-TWT consists of a magnetron injection gun (MIG, operated in the temperature – limited region) that produces an annular beam, an interaction region placed at the centre of a strong magnet, and an RF extraction region. When a pulsed or continuous potential is applied on the anode of the particle emitter (MIG), an electric field is created at the cathode and the electrons, at an angle with the tube axis, are drawn off the annular strip on the lateral face of a convex thermionic dispenser cathode. The cathode and anode are positioned with respect to the magnetic lines in such a way that the electric field at the cathode has both

perpendicular and parallel components. Initially, the electrons are randomly distributed in phase over the range (0, 2π) and are assumed to make a uniform current density over the surface area of the interaction region. The cyclotron frequency of electrons is always kept slightly less than the R.F. wave, so that the bunch of electrons feels retardation continuously and transfer significant amount of kinetic energy to the R.F. wave. As a result, emitted electrons first move azimuthally along cycloidal trajectories over the cathode surface [Nusinovich (2004)]. Under the action of electric field component, which is parallel to the magnetic force line, they become accelerated and thus leave the gun region. Therefore, the electrons acquire both orbital and axial velocity components and gyrate helically about a fixed guiding centre, where the radius of the path, the Larmor radius, is small compared to the radius of the beam, so that the beam radius remains annular as it propagates. One of the most important issues in MIG is the electron's velocity spread which is limiting factor of the device. The reasons for this are the space charge, initial thermal velocity spread, emitter roughness, and in-homogeneity of external fields in the region of emitters having a finite width. The gyro-TWT suffers from instabilities and self-start oscillations due to backward waves. The interaction circuit consists of a long region supporting an electromagnetic mode to interact with the electron beam. The interaction circuit in gyro-TWT is a smooth wall conventional cylindrical waveguide. The electrons move towards along the interaction circuit under the influence of the DC magnetic field. Due to adiabatic invariance of the magnetic momentum, $p_{\perp}^{2} / B$=constant, the electron orbital momentum increases. In the interaction circuit, the magnetic field is uniform and electrons interact with the chosen rotational electric TE_{mn} waveguide mode and give rise to amplification. The wave propagates along the waveguide axis with the phase velocity of

$v_p = \omega / k_z$ and a group velocity of $v_g = d\omega / dk_z$. These velocities are related as $v_p v_g = c^2$. The spent beam of electrons enters a magnetic decompression region and diverges off the axis to settle on the collector surrounding the beam. The amplified RF output is extracted axially through the output window that is vacuum sealed to the tube. In the case of radial extraction the RF output power is converted into a Gaussian beam with the use of a built-in mode converter before the extraction through the window. To couple the desired mode inside the waveguide and to extract amplified wave, input and output couplers are used. Depending on the operating mode and wavelength, various types of couplers can be used.

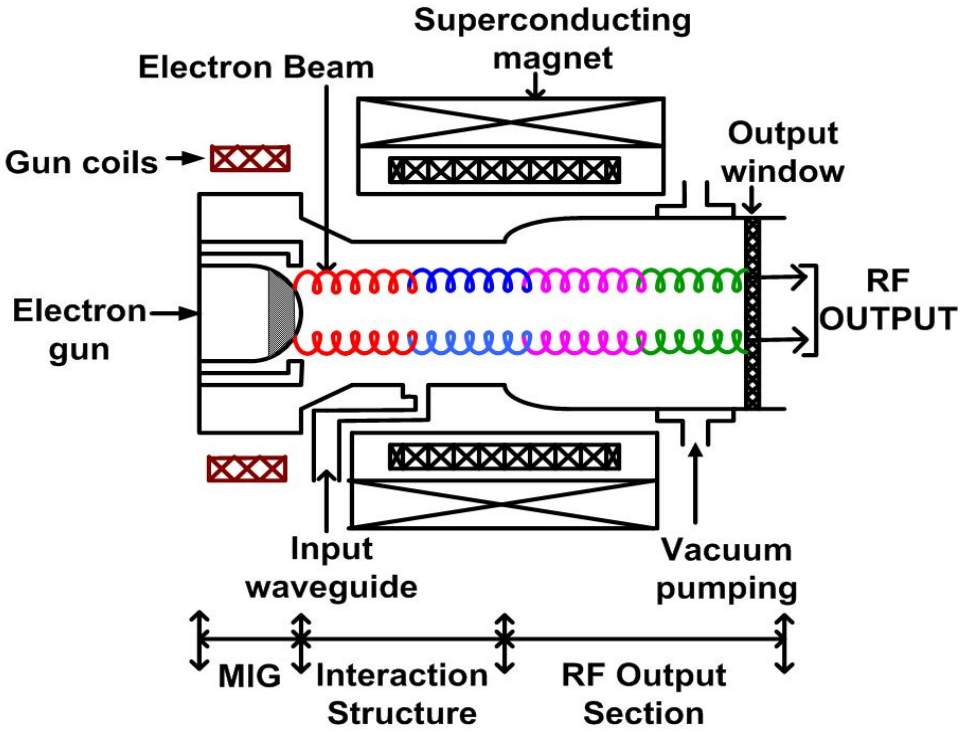

Figure 2.4. Schematic of a Gyrotron Traveling Wave Tube Amplifier.

2.5.1. Working Principle

When an indirectly heated cathode ring in the electron gun emits an annular beam of electrons by thermionic emission enters in the interaction circuit (cylindrical waveguide) of

gyro-TWT, the electric field produces a force on electrons as they adiabatically spiral around the external applied DC magnetic field lines. A key factor in beam-wave interaction is the ratio of perpendicular velocity, v_t to axial velocity v_z. Usually v_t / v_z is in the range of 1.0 to 2.0. The lower value gives greater stability against spurious oscillation while the high value gives greater fficiency. Electron transverse velocity comes from the magnetic effect. The Larmor radius of the beam is determined by relativistic mass of electron and magnetic field. The microwave frequency of the device and the magnitude of an applied dc magnetic field are closely related by the synchronism condition. The point of grazing interaction, where the two curves just touch, is the usual point of operation. Gyro-TWT can not built at very low beam voltage because its gain, bandwidth and output power decrease rapidly with beam power. This force not only changes the phase of the electrons as their orbits are slowed down and speeds up, but it alters the perpendicular momentum of the electrons in a relativistic manner, resulting in a non-uniformly distributed electron density through the process of bunching. In this process, a majority of electrons are made to gyrate coherently thus driving the fluctuating current density term in Maxwell's equations and efficiently transferring energy from the electrons to Electromagnetic fields. As the electron beam travels down a long interaction circuit, this bunching effect grows, amplifying the electric fields. A beam that is more highly bunched becomes a larger source of fluctuating current and hence gives up more of its energy to EM field. Eventually, the electrons loose so much of energy due to decreases in relativistic mass hence the cyclotron frequency shifts and they no longer interact. Energy is no longer efficiently extracted from the beam and nonlinear saturation has set in. However, if the beam is allowed to evolve too long, or if the bunching process is forced too strongly, an over bunching may result in

which the electrons again take energy from the RF fields in the interaction circuit, resulting in a dramatic efficiency drop. Finally, the spent electron beam is collected by a collector, where the beam dissipates on a smooth wall. The radiation frequency in CRMs is at either the cyclotron frequency or at one or many of its harmonics. Thus the radiation frequency is not entirely controlled by the size and shape of the waveguide or the resonator. The RF power propagates out of the interaction circuit and travels down the collector (having good thermal conductivity) in a TE_{mn}-like mode, and then passes through the glass output window. The use of a higher order Gaussian like mode significantly simplify the design of the internal mode converter and allow an easy formation of a Gaussian beam at the window for an efficient coupling to the HE_{11} mode of a corrugated waveguide for an ultra low loss transmission to the antenna of a radar or a communication system.

2.6. Applications of Gyro-TWT Amplifier

Gyro-TWT can be used for a number of applications, such as ultra-high resolution radars, imaging radars, magnetic resonance imaging, high density communication systems, spectroscopy, study of cloud tomography, linear accelerators, etc. As the attenuation coefficient of the atmosphere increases with frequency, the existing communication system is required to be enhanced and changed to meet the future demand of the high information density communication systems, and provide high powers for the millimetre wave radars for their enhanced range and resolution. The millimetre wave radars enjoy the advantages of both the microwave radar and laser radar. Compared to the microwave wave radar, millimetre wave radar has advantages such as narrow beam width, high resolution, multipath effects and anti-jamming capability, smaller size and light weight. It can more effectively work in the rain, fog, and battlefield smoke work environment, compared with

infrared and optical radars. Research in this area is mainly focused at frequencies of about 35 GHz and 94 GHz, due to availability of the two atmospheric windows at these frequencies. The gyro-TWT devices applications span a wide range of technologies such as point-to-point communication, satellite communication, satellite-to-home communication, military radar (missile guidance, missile tracking), civilian radar (weather detection, highway collision avoidance, airport traffic control, speed detectors, air-traffic control, mapping of ground terrain, remote sensing), Dynamic nuclear polarization (DNP) and Electron paramagnetic resonance spectroscopy, etc. On the other hand, conventional lasers and Free Electron Lasers (FEL), which dominate the far infrared and the optical regimes, suffer from low efficiencies and heavy in the millimeter wave regime.

2.7. Different Types of RF Circuits for Gyro-TWT Amplifier

2.7.1. *Dielectric load*

By loading with dielectric, the propagating mode in the waveguide can be made less dispersive, i.e., the group velocity of the wave is essentially constant for a wide range of propagation constants except near the cut-off. By choosing optimised parameters of electron beam, the electrons can be made resonant with the wave across a wide range of frequencies, leading to a broadband amplifier. The disadvantage of this process is that the dielectric loading at higher frequency is difficult due to miniaturization and also dielectric materials are unable to handle high power with such miniaturization.

2.7.2. *Tapered Waveguide*

It was shown theoretically that a broadening of the amplification band in a tapered circuit device with a tapered magnetic field could be realized. Theoretically, a large bandwidth can be obtained by using a tapered interaction cirucit with an axially tapered

magnetic field profiled to maintain synchronism. The shorter effective interaction length of the tapered gyro-TWT amplifier increases the start-oscillation current of the absolute instability. Thus, the reflective instability due to output mismatch becomes the dominant source of spurious oscillation, rather than absolute instability as in a uniform interaction circuit. At low voltage, the electron cyclotron resonance interaction occurs very near the local cut-off of the interaction circuit where the interaction impedance is strong and relatively insensitive to beam velocity spread.

2.7.3. *RF Circuit with Helical Corrugation*

A helical corrugation which scatters the operating near cutoff mode into a traveling wave resulting in one-way output from the cavity has also been used. The use of a helix mounted into the cylindrical conducting waveguide for improvement of gyro-TWT wave dispersion has been reported earlier. If the corrugation amplitude '*l*' is small compared with the wavelength, the field structure and dispersion characteristics of a helical waveguide can be calculated by means of the method of perturbation. When using the helical waveguide as an RF circuit in gyro TWT, it is advantageous to have an amplification parameter, which is proportional to electron current, much smaller than the coupling coefficient.

2.7.4. *Photonic Band Gap Waveguide*

Conventional high-power microwave vacuum electron devices operate at fundamental modes. As the operating frequency increases to the millimeter or sub-millimeter wave range, the dimension of the interaction circuit becomes too small. This makes the accurate fabrication of the circuit is difficult and expensive and the heat load per unit area on the circuit walls excessive. It is also very difficult to pass an electron beam through such small structures without beam interception. In addition, for higher power

operations, a larger interaction circuit is needed for better thermal dissipation of radio frequency (RF) power. The PBG structures are periodic lattices of dielectric, metal or composite arrangement and which are transparent (pass) for certain band of frequencies and opaque (stop) for the rest of frequencies [Sirigiri *et al.* (2001)]. The local defects in photonic crystals can be used to localize the electromagnetic fields within the frequency gap of the unperturbed photonic crystals. The localized mode frequency depends on the exact nature of the local defect. The defect in PBG structures can be used to guide electromagnetic signals, to create frequency-selective waveguides by properly designing the nature of the repeated defect. This mode selective property of PBG structures gives us an edge to work at higher order mode while avoiding mode competition without significantly perturbing the operating mode. The overall effective area of the device increases which gives the advantage of the ease of fabrication at higher frequencies.

2.8. Gyro TWT ─ A Review

The CRM based devices notice in late 1950s, physics behind the beam-wave interaction mechanism using linear analysis has been reported in the early 1960s and in the mid of 1960s, the first outline of nonlinear analysis was reported [Zhurakhovskiy (1964)]. The non-linear analysis for gyro-TWT has been reported by [Sprangle and Dorbot (1977), Chu *et al.* (1979), Chu *et al.* (1980)] and subsequently, non-linear analysis of relativistic gyro-TWT has been developed in early 1980s [Bratman *et al.* (1981), Fliflet *et al.* (1986)]. The inital work on gyro-TWT done by Chu in 1977 at Novel Research Laboratory (NRL) using linear theory and a numerical simulation code which form the basis of theoretical calculations [Chu *et al.* (1979)]. Most of these experiments have used the fundamental mode in a circular waveguide to improve the problems of mode competition. At higher

frequencies all though transverse dimension is less so that waveguide fabrication (thermal damage), mode competition problem is also occur. In 1979 Seftor demonstrated first experimental gyro-TWT with an operating frequency of 35GHz at the NRL and achieved a output power of 10kW and an stable gain of 17dB. At NRL demonstrated an experiment for the gain enhancement and stability improvement of this amplifier by employing a resistively loaded interaction circuit. This experiment result was 42dB saturated gain, 3.2 kW power, 1.5% efficiency with a 3dB bandwidth of 2% [Barnett *et al.* (1980)]. In 1981, Lau *et al.* have investigated the instability due to oscillations in gyro-TWT using cold/warm beam in a lossless/lossy waveguide circuit [Lau *et al.* (1981)]. In 1981, Varian associates reported a C-band dominant circular electric mode gyro-TWT experiment that produced 120kW power, 26% efficiency, 18dB saturated gain with a 3dB bandwidth of 6% at [Symons *et al.* (1981), Fergusion *et al.* (1981)]. In 1981, 94GHz gyro-TWT predicts 28kW output power, 8% efficiency, 30dB gain, and a band width of 8% [Eckstein *et al.* (1981)]. A 95GHz gyro-TWT yield 15kW output power, 6.2% efficiency, and 30dB gain with 1.6% bandwidth [Grantstein and Alexeff (1987).

A linear theory using Laplace transform explain the physical understanding of the mechanisms of the various spontaneous oscillation of high power harmonic Gyro-TWT and also describe linear analysis fails in saturation region where nonlinearities is important [Kou *et al.* (1992)]. Nonlinear analysis and design of high power harmonic gyro-TWT proof that the high harmonic gyro-TWT has high start oscillation current and generate high output power then fundamental harmonic, predicts output power of three stage second harmonic 533kW, efficiency 21.3%, and 7.4% saturated gain [Wang *et al.* (1992)]. In 1994, Leou have studied two (Ka-band and W-band) stable three section high power gyro-TWTs

using attenuating sever in its RF sections operating in a low-loss TE_{01} mode for their stability improvement. These configurations yielded a peak power of 230kW at 35GHz with 23% efficiency, 46dB gain and 105kW at 94GHz with 21% efficiency, 45dB saturated gain, respectively [Leou 1994]. Simultaneously, two stable Megawatt classes of harmonic TE_{31} mode gyro-TWTs operating at 140GHz with axis encircling beam from a cusp gun and a magnetron injection gun (MIG) for the output powers of 775kW and 937kW with 15.5% and 18.7% efficiency, saturated gains of 27dB and 30dB respectively have been studied [Wang *et al.* (1994)]. In 1996, a 3rd harmonic gyro-TWT using a slotted RF circuit for its stability at 95GHz. This developed an output power of 30kW, 20% efficiency, and 40dB saturated gain for an axis-encircling beam of 6% axial velocity spread [Chong *et al.* (1996)]. Consequently, the first experimentation of a slotted 3rd harmonic gyro-TWT at X-band was reported as a scaled proof-of-principle test of the 95GHz multi-section slotted amplifier under development at CPI. They reported the effect of sever in a two-stage W-band Gyro-TWT using slotted RF sections [Zhang *et al.* (1998)].

A detailed physics and experimental verification of gyro-TWT amplifier were reported [Chu *et al.* (1990), Chu *et al.* (1995), and Chu *et al.* (1999)]. After the successful experimental verification, the investigation of mechanism of oscillations and instabilities were carried out through a detailed modelling of the interaction circuit and the development of methods of their suppression led to a significant step toward the realization of the potential of a gyro-TWT. At National Tsing Hua University (NTHU), Taiwan experimentally demonstrated a Ka-band gyro-TWT that developed 18.4kW power, with an electronic efficiency of 18.6% and bandwidth of ~10% [Chu *et al.* (1989)] and next, a millimetre wave gyro-TWT employing a sever was experimented in order to improve the

stability and that produced 27kW power, 35dB saturated gain, 16% efficiency with 7.5% bandwidth [Chu *et al.* (1990)]. In 1995, NTHU employed distributed wall section to make the efficient study of oscillation suppression and obtained 62kW power, 33dB saturated gain, 21% efficiency and 3dB bandwidth of 12% at 35GHz [Chu *et al.* (1995)]. Absolute instability investigates by simulation approach and predicts that the distribution loss is more effective then severed loss. Ka-band produced power 62kW, 21% efficiency, and 12% bandwidth with a 33dB gain [Chu *et al.* (1995)]. An early 94GHz, gyro-TWT produce 20kW output power, 8% efficiency, 30dB saturated with 3dB bandwidth of 2% [Granatstein *et al.* (1997)]. The 95GHz gyro-TWT amplifier are reported for a slotted third-harmonic yield 6kW output power, 5% efficiency, 11dB saturated gain with 3% bandwidth [Chong *et al.* (1998)]. Study of instability and suppression of spontaneous oscillation by distributed wall losses, perdicts output power 93kW, 26.5% eficiency, and 70dB gain and with a 3GHz bandwidth [Chu *et al.* (1999)].

A mode selective second harmonic W-band produce 600kW, with an efficiency of 24%, 30dB saturated gain and a 3dB bandwidth of 2.7% [Wang *et al.* (2000)]. A 95GHz gyro-TWT yield 28kW output power 8% efficiency, 31dB saturated gain [Granatstein *et al.* (2001)]. Design a heavy loaded W-band gyro-TWT amplifier for high power and broad-band capability [McDermott *et al.* (2002)], produce saturated gain 140kW with 5% velocity spread, 28% efficiency, 50dB saturated gain and a 3dB bandwidth 5% [Song *et al.* 2004]. Zhang and his group have studied a gyrotron-traveling wave amplifier using co-axial waveguide as a mode selective RF structure at millimeter and submillimeter wave frequencies for high power, and ultrahigh gain [Zhang *et al.* (2004)]. This nonlinear simulation study predicted a few tens of kilowatts with an ultrahigh gain of ~67dB for a

coaxial-waveguide mode of $TE_{28,\ 16}$ at fundamental 140GHz. Communication and Power Industries (CPI) demonstrate a W-band gyrotwystron produced output power of 60kW, 34dB saturated gain, 15% efficiency with bandwidth of 1.6GHz and gyroklystron produced 100kW power, 35dB saturated gain, 30% efficiency and bandwidth of 0.7GHz [Blank *et al.* (1999), Blank *et al.* (2002)] .The mode competition in gyro-TWT is sophisticatedly connected to instabilities, circuit losses, and reflective feedback. In the last of 20th century the physical origins of spurious oscillations were reported and characterized by Chu and his group at NTHU. The basic knowledge of these processes leads to the concept of an ultra high gain scheme which employs distributed wall losses for the suppression of spurious oscillations. A proof-of-principle Ka-band, TE_{11} mode stable gyro-TWT experiment at zero drive has produced 93kW saturated peak power with the gain of 70dB and a 3dB bandwidth of 3GHz [Chu *et al.* (1999)]. At the beginning of 21st century at NRL, Nguyen and his group designed a Ka-band TE_{11} mode gyro-TWT with high thermal conductivity ceramic elements that produced 78kW power, 60dB saturated gain, 19% efficiency with a 3dB bandwidth of 17.1% [Nguyen *et al.* (2001)]. Further, in 2002 Graven and his group experimentally demonstrated a Ka-band lossy ceramic loaded TE_{01} gyro-TWT which developed 137kW power, 47dB saturated gain, 17% efficiency with a 3dB bandwidth of 3.3% [Graven *et al.* (2002)]. A 96GHz yield more then 0.5kW with 45dB gain and bandwidth of 8GHz [Blank *et al.* (2005)].

During the last two decades, many computer codes have been developed and used for the analysis and design of the gyro-TWT [Nguyen *et al.* (2001)]. Analyse of multi-stage gyro-TWT by using self consistent code, yield 155kW output power, 15% efficiency, and 45dB gain with 2.2GHz bandwidth [Yeh *et al.* 2003] at 32.9GHz when the velocity spread

is 5%. W-band 2nd harmonic multistage gyro-TWT and obtained a peak power of 215kW at 89.9GHz with ~ 14% efficiency, and 60dB saturated gain for a 100kV, 15A electron beam with an axial spread of 5% [Yeh *et al.* (2004)]. Tsai and his group have examined theoretically, the diversity of the absolute instability behaviour and physical processes involved in a W-band gyro-TWT using distributed wall losses [Tsai *et al.* 2004)]. Nevertheless, more recently, numerical techniques, like, finite difference time domain (FDTD) method, finite integration (FI) method, etc. have been used for modelling and simulation of such devices.

PIC simulation of 35GHz, 150kW gyro-TWT has been carried out by Reddy and his group using an FI based algorithm in 2010 [Reddy *et al.* (2010)]. Du and his group have studied a millimeter wave gyro-TWT with high stability using a lossy mode selective dielectric-lined (DL) waveguide [Du *et al.* (2010)]. Xu and his group have studied a Ka-band gyro-TWT using distributed loss technique for 100kW peak output power, bandwidth of 1.8GHz, electronic efficiency of 23.8%, and the gain of 56dB [Xu *et al.* (2010)]. A W-band produced 278.2kW output power, 22.4% saturated efficiency, 69dB gain with 3dB bandwidth of 5.08% [Chiu *et al.* (2010)]. Analysis of instability and predicts 160kW output power, 22.8% efficiency 40dB gain with 5% 3dB bandwidth [Wang *et al.* (2011)]. Shou-Xi Xu and his group have studied the beam wave interaction mechanism in a Ka-band gyro-TWT including a severed structure using a particle in cell code (FDTD based). The amplifier outputs a peak power of 155kW with a power conversion efficiency of 22% using 70kV, 10A electron beam [Xi Xu *et al.* 2011].

Bentian Liu and his group design Ka- band TE_{01} gyro-TWT at the fundamental cyclotron harmonic with periodic dielectric loaded circuit is used in the interaction circuit

of the gyro-TWT to suppress unwanted modes with zero-drive stable at operating obtained saturated peak power of 156 kW, gain 44dB with efficiency of 23.3% and bandwidth of 1.8GHz [Liu *et al.* (2011)]. Chien-Lun Hung at National Penghu University (NPU) achieve stability for second harmonic by applying distributed losses on the inner and outer wall, coaxial gyro-TWT produces a peak power of 293kW in the ka-band with a efficiency of 21%, a saturated gain of 42dB and a 3dB bandwidth is 1.31GHz [Hung *et al.* (2012)] and Ran Yan and his group design a Q-band gyro-TWT loaded with periodic rings of lossy dielectric operating in the circular TE_{01} mode at the fundamental cyclotron harmonic gives peak output power of 152kW, saturated gain 41dB, and 21.7% efficiency at 47.6GHz with zero drive stable at operating point [Yan *et al.* (2012)] and for suppression of spurious oscillations Efeng Wang and his group in 2012 the designed and employed a periodic lossy-material-loaded circuit in our experimental study of TE_{01} Ka-band gyro-TWT and obtained peak power of 290kW was measured with maximum gain 56dB, 3dB bandwidth 2.1GHz, and 34.2% efficiency [Wang *et al.* (2012)] and Yanyan Tian and his group shows a compact and novel slow-wave structure (SWS) called the folded rectangular groove guide is produce output power of over 260W with a sheet electron beam in the 3dB bandwidth range of 88.5–98.5GHz [Tian *et al.* (2012)] and Y.S.Yeh and his group shows for reduce magnetic field and decrease wall losses due to global reflective oscillation, W-band gyro-TWA is predicted a peak output power of 111kW at 98GHz with saturated gain of 26dB and an efficiency of 25%, and a 3dB bandwidth of 1.6GHz [Yeh *et al.* (2012)].

Two-stage circuits can increase the stability threshold as well as provide other advantages. The researcher of NRL group employed a sophisticated circuit comprised of two-stage tapered rectangular interaction sections isolated by a short cut-off section. The

input signal was preamplified in the first stage. The wave was then reflected at the cut-off section, while the imbedded signal in the electron beam was amplified again in next stage, C.L. Hung and his group in shows for enhance stability and increase bandwidth two-stage tapered gyro-TWT amplifier with distributed-loss method is used, predicted to produce a peak power of 60kW with an saturated gain of 52dB and a efficiency of 29% in the Ka-band with bandwidth around 5.7GHz [Hung *et al.* (2012)]. In 2013, Chao Hai Du and his group designed a W-band TE_{01} mode gyro-TWT pulse prototype for high gain and broadband capabilities, amplifier's highest efficiency of 32.4%, and the bandwidth of 4.2GHz with output power 50kW [Du (2012)]. The analytical and PIC simulation of a Ka-band gyro-TWT amplifier has been studied for its beam-wave interaction behaviour by Thottappan and his group, in which ~135kW saturated RF power with a saturated gain of ~41dB and a conversion efficiency of ~23% has been reported. This study includes the effect of velocity spread on the performance of the device [Thottappan *et al.* (2013)].

In 2014, Ran Yan and his group design a W-band zero-drive stable gyro-TWT loaded with non-uniform periodic lossy dielectric rings is operating in the circular TE_{01} mode circuit at the fundamental cyclotron harmonic produces peak output power 112kW with a 69.7dB saturated gain and 23.3% efficiency at 93.5GHz [Yan *et al.* 2014]. A low voltage W-band gyro-TWT for a saturated RF output power of ~43kW with a gain of 54dB and a 3dB bandwidth of 3.7GHz was reported by Li and his group [Li *et al.* (2014)]. In 2014, Yong Tang and his simulate a W-band gyro-TWT loaded with periodic lossy dielectric produces a peak output power of 198kW, saturated gain of 62.3dB with efficiency of 28.3% at 92.5GHz [Tang *et al.* (2014)] and Wei Jiang and group produce to design for enhance the power handling capability, curved collector for a *Q*-band gyro-TWT

results shows the average dissipated power density of 0.162 kW/cm^2 is 64% of that in the cylindrical collector [Jiang *et al.* (2014)] and Yong Tang and his design of a novel dual-band (Ku/Ka) gyro-TWT gain per-unit of the Ku-band is lower than Ka-band's, maximum output power of 238/158 kW, maximum gain of 45.5/50.4 dB, and 3dB bandwidth ~2.1/3.4 GHz, respectively, for Ku-band and Ka-band, the device has a bandwidth of 1.5/2.5 GHz for Ku/Ka-band with a peak power >100kW [Tang *et al.* (2014)] and Yinfu Hu and his group design and developed high power, wide bandwidth W-band (TWT) is covers folded waveguide (FWG) circuit, give 30W output power in frequency between 91 and 101GHz with over 30dB saturated gain here maximum power was found to be about 40W at 95GHz [Hu *et al.* (2014)]. Wang and his group have simulated a Ku-band gyro-TWT that produced ~153kW with 2.3GHz bandwidth, ~41dB saturated gain and an efficiency of ~20% [Wang *et al.* (2014)]. In 2015, Elizabeth J. Kowalski and her group MIT built, a 94GHz overmoded travelling-wave tube, operates in the rectangular TM_{31} mode of the cavity, 28dB and the saturated output power 100W, bandwidth of 30MHz [Kowalski *et al.* (2015)].

Using helically corrugated waveguide produces a peak pulse output power 144.8kW when the average input power is 5.8kW with an efficiency of 66.3% [Zhang *et al.* (2015)]. For eleminating the mode copetition using PBG by analytical pridect output power around 91kW, efficiency around 13% with a gain of 40dB and though simulation yield around 90kW with an bandwidth of around 14% [Thottappan *et al.* (2016)]. By using a helically corrugated waveguide yield 6kW continuous output power with a bandwidth of 2.1GHz [Samsonov *et al.* (2016)].The specifications of the gyro-TWTs developed, in 1980's, 1990's, 2000's and 2010's, at some typical laboratories are given in Appendix 1.

Appendix 1: Specifications *of Gyro-TWT developed in some typical Laboratories*

Operating Frequency (GHz) / band	**Power (kW)**	**Efficiency (%)**	**Gain (dB)**	**% bandwidth/ 3-dB bandwidth (GHz)**	**Mode/ Loading/ Tapering**	**Reference/Year**
35	100	>10	17	~ 10	—	Seftor *et al.* (1979)
35.1	—	—	32	—	—	Barnett *et al.* (1979)
35.12	3.2	—	42	—	Circular TE_{01} Resistive wall loading	Barnett *et al.* (1980)
5.2	128	24	20	7.25	Circular TE_{11} Tapered magnetic field	Ferguson *et al.* (1981)
35	—	—	18	13	Circular TE_{01} Tapered cross section and magnetic field	Barnett *et al.* (1981)
Ka-band	18.4	18.6	18	10	Tapered interaction structure	Chu *et al.* (1990)
Ka band (33.5GHz)	27 (Peak)	16	35	2.5	Circular TE_{11}	Chu *et al.* (1990)
35	5	10	20	33	Rectangular Tapered cross section	Park *et al.* (1991)

Operating Frequency (GHz) / band	Power (kW)	Efficiency (%)	Gain (dB)	% bandwidth/ 3-dB bandwidth (GHz)	Mode/ Loading/ Tapering	Reference
9-11	80	30	15	20	Rectangular Dielectric loaded	Leou *et al.* (1992)
35	7.4	15	30	8	—	Park *et al.* (1993)
Ka-band (27-38 GHz)	—	10	25	33	Two-stage	Park *et al.* (1994)
35	8	16	25	20	Two-stage tapered cross section	Park *et al.* (1995)
34.2	62	21	33	12	—	Chu *et al.* (1995)
16.7	207	—	—	—	Circular TE_{21} Axially sliced	Wang *et al.* (1996)
X-band	55	11	27	11	Rectangular TE_{10} Dielectric loaded	Leou *et al.* (1996)
X-band	55- 75	—	30	20	Rectangular Metal disc-loaded	Leou *et al.* (1998)
95	6	5	11	3	Slotted structure	Chong *et al.* (1998)
Ka-band	93 peak	26.5	70	3 GHz (3-dB)	Lossy section	Chu *et al.* (1998)
X-band	1×10^3	20	23	—	Helical waveguide	Denisov *et al.* (1998)
—	—	28	38	19	Helical waveguide	Denisov *et al.* (1998)

Operating Frequency (GHz) / band	Power (kW)	Efficiency (%)	Gain (dB)	% bandwidth/ 3-dB bandwidth (GHz)	Mode/ Loading/ Tapering	Reference
—	—	—	29 Peak	10	Helical waveguide	Cooke and Denisov (1998)
35	2×10^3	20	30 Saturated	3.5	Circular TE_{41} Sliced waveguide	McDermott *et al.* (1998)
Ka-band	100	26.5	70	8.6	Circular TE_{11} Lossy graphite covered wall	Chu *et al.* (1999)
35	93 Saturated	26.5	70	8.6	Circular TE_{11}	Chu *et al.* 1999
9.2	1.1×10^3	29	37 Saturated 47Linear	21	Helically waveguide	Bratman *et al.* (2000)
91.4	600	24	30	2.7	Circular TE_{02}	Wang *et al.* (2000)
Ka-band	57.9-92.2	-	36.0-57.1	2.5-3.7 1 dB below saturation	Circular Diffractive loading Distributed loss	Nguyen *et al.* (2001)
92	140	28	50 (Saturated)	5	Circular TE_{01} Distributed-loss circuit	McDermott *et al.* (2001)
35	137 (Saturated)	17	47	3.3	Circular TE_{01} Ceramic rings (Distributed attenuation)	Garven *et al.* (2002)
32.9	155	15	45	2.2 GHz (3-dB)	Multistage	Yeh *et al.* (2003)
140	30 (Peak)	12	29	2.3 GHz (3-dB)	Confocal waveguide HE_{06}	Sirigiri *et al.* (2003)

Operating Frequency (GHz) / band	Power (kW)	Efficiency (%)	Gain (dB)	% bandwidth/ 3-dB bandwidth (GHz)	Mode/ Loading/ Tapering	Reference
34.2	—	10	23.8	4.1	Rectangular Two-stage tapered cross section	Baik *et al.* (2003)
Ka-band 31.8-36	>3 kW	—	< 20 dB/m	4	Two-stage tapered cross section (Frequency multiplication)	Baik *et al.* (2004)
Ka-band	435	31	45	~ 5.8	Coaxial waveguide	Hung and Yeh (2005)
W-band (96)	≥ 0.5	—	≥ 45	≥ 8 GHz (3-dB)	Circular TE_{01}	Blank *et al.* (2005)
—	62	21	33 Saturated	12	Distributed losses	Leou *et al.*
Ka-band	50	20	30	3%	Circular TE_{21}^{2} mode-selective circuit	Harriet *et al.* (2007)
Ka-band	86	21.3	33	6%	Circular TE_{01} mode-selective circuit	Liu *et al.* (2010)
Ka-band	156	23.3	44	1.8	circular TE_{01} periodic lossy dielectric loading	Liu *et al.* (2011)

Operating Frequency (GHz) / band	Power (kW)	Efficiency (%)	Gain (dB)	% bandwidth/ 3-dB bandwidth (GHz)	Mode/ Loading/ Tapering	Reference
Ka-band	160	22.8	40	5%	Circular TE_{01} Lossy interaction circuit	Wang *et al.* (2011)
47.6	152	21.7	41	2	periodic lossy dielectric rings	Yan *et al.* (2012)
Ka-band	290	34.2	56	2.1	periodic lossy dielectric loading	Wang *et al.* (2012)
W-band	>50	32.4	55	4.2	Circular TE_{01} Lossy ceramic	Du *et al.* (2013)
W-band	90	23.3	69.7	4	nonuniform periodic lossy dielectric rings,5%	Yan *et al.* (2014)
Ku-band	153	20	41	2.2	loaded with lossy ceramic rings	Wang *et al.* (2014)
U-band/ 48GHz	158	22.6	47.4	3.2	periodic loaded dielectric	Xu *et al.* (2015)
Ku-band	420	23	35	1.6	Circular TE_{01} lossy ceramic mode selective loss	Wang *et al.* (2015)
K-band	9kW			2.1GHz	TE_{11} Helical waveguide	Samsonov *et al.* (2016)

2.9. CONCLUSION

In this chapter, the development of high-power microwave sources and their limitations has been reviewed. Various approaches of classifying the microwave sources have also been discussed. The evolution of microwave sources is started from triode and concluded at fast-wave gyro devices. Fast-wave gyro devices and different gyro-amplifiers (gyro-TWT, gyroklystron and gyro-Twystron) have been discussed. Working principle of gyro-TWT and its different application have been presented. Different types of interaction region in gyro-TWT (Dielectric loaded waveguide, Tapered waveguide, RF circuit with Helical corrugation and PBG waveguide) used for enhancing the device output performance have been described. A detailed literature review for the gyro-TWT device development, present status, issues and limitations have also been presented.

In the next chapter, the detailed nonlinear single mode time independent analysis of gyro-TWT using single particle theory will be presented. Further, the developed analysis is benchmarked with the reported experimental results.